Study of $B \to p\bar{p}\pi\pi$

K. Chu,[58] M.-Z. Wang,[58] I. Adachi,[16,12] H. Aihara,[78] S. Al Said,[74,35] D. M. Asner,[2] V. Aulchenko,[3,62] T. Aushev,[51] R. Ayad,[74] V. Babu,[7] I. Badhrees,[74,34] S. Bahinipati,[21] A. M. Bakich,[73] P. Behera,[24] C. Beleño,[11] J. Bennett,[49] V. Bhardwaj,[20] B. Bhuyan,[22] J. Biswal,[31] A. Bobrov,[3,62] G. Bonvicini,[81] A. Bozek,[59] M. Bračko,[46,31] M. Campajola,[28,54] L. Cao,[32] D. Červenkov,[4] P. Chang,[58] V. Chekelian,[47] A. Chen,[56] B. G. Cheon,[14] K. Chilikin,[42] H. E. Cho,[14] K. Cho,[37] S.-K. Choi,[13] Y. Choi,[72] S. Choudhury,[23] D. Cinabro,[81] S. Cunliffe,[7] N. Dash,[21] F. Di Capua,[28,54] S. Di Carlo,[40] Z. Doležal,[4] T. V. Dong,[10] S. Eidelman,[3,62,42] D. Epifanov,[3,62] J. E. Fast,[64] T. Ferber,[7] A. Frey,[11] B. G. Fulsom,[64] R. Garg,[65] V. Gaur,[80] N. Gabyshev,[3,62] A. Garmash,[3,62] A. Giri,[23] P. Goldenzweig,[32] B. Golob,[43,31] O. Hartbrich,[15] K. Hayasaka,[61] H. Hayashii,[55] W.-S. Hou,[58] C.-L. Hsu,[73] T. Iijima,[53,52] K. Inami,[52] A. Ishikawa,[16,12] R. Itoh,[16,12] M. Iwasaki,[63] Y. Iwasaki,[16] W. W. Jacobs,[25] H. B. Jeon,[39] Y. Jin,[78] D. Joffe,[33] K. K. Joo,[5] G. Karyan,[7] T. Kawasaki,[36] D. Y. Kim,[71] S. H. Kim,[14] K. Kinoshita,[6] P. Kodyš,[4] S. Korpar,[46,31] P. Križan,[43,31] R. Kroeger,[49] P. Krokovny,[3,62] R. Kulasiri,[33] Y.-J. Kwon,[83] Y.-T. Lai,[16] I. S. Lee,[14] S. C. Lee,[39] L. K. Li,[26] L. Li Gioi,[47] J. Libby,[24] K. Lieret,[44] D. Liventsev,[80,16] T. Luo,[10] M. Masuda,[77] D. Matvienko,[3,62,42] M. Merola,[28,54] K. Miyabayashi,[55] R. Mizuk,[42,51] G. B. Mohanty,[75] T. Mori,[52] R. Mussa,[29] E. Nakano,[63] T. Nakano,[67] M. Nakao,[16,12] K. J. Nath,[22] M. Nayak,[81,16] N. K. Nisar,[66] S. Nishida,[16,12] K. Nishimura,[15] H. Ono,[60,61] Y. Onuki,[78] P. Oskin,[42] P. Pakhlov,[42,50] G. Pakhlova,[42,51] B. Pal,[2] T. Pang,[66] S. Pardi,[28] C. W. Park,[72] H. Park,[39] S.-H. Park,[83] S. Paul,[76] T. K. Pedlar,[45] R. Pestotnik,[31] L. E. Piilonen,[80] V. Popov,[42,51] E. Prencipe,[18] M. T. Prim,[32] P. K. Resmi,[24] M. Ritter,[44] A. Rostomyan,[7] N. Rout,[24] G. Russo,[54] D. Sahoo,[75] Y. Sakai,[16,12] S. Sandilya,[6] L. Santelj,[16] V. Savinov,[66] O. Schneider,[41] G. Schnell,[1,19] J. Schueler,[15] C. Schwanda,[27] Y. Seino,[61] K. Senyo,[82] M. E. Sevior,[48] C. P. Shen,[10] J.-G. Shiu,[58] E. Solovieva,[42] M. Starič,[31] Z. S. Stottler,[80] T. Sumiyoshi,[79] W. Sutcliffe,[32] M. Takizawa,[70,17,68] U. Tamponi,[29] K. Tanida,[30] F. Tenchini,[7] T. Uglov,[42,51] Y. Unno,[14] S. Uno,[16,12] P. Urquijo,[48] Y. Usov,[3,62] G. Varner,[15] A. Vinokurova,[3,62] A. Vossen,[8] B. Wang,[47] C. H. Wang,[57] P. Wang,[26] X. L. Wang,[10] J. Wiechczynski,[59] E. Won,[38] S. B. Yang,[38] H. Ye,[7] J. Yelton,[9] J. H. Yin,[26] Y. Yusa,[61] Z. P. Zhang,[69] V. Zhilich,[3,62] V. Zhukova,[42] and V. Zhulanov[3,62]

(Belle Collaboration)

[1]*University of the Basque Country UPV/EHU, Bilbao 48080*
[2]*Brookhaven National Laboratory, Upton, New York 11973*
[3]*Budker Institute of Nuclear Physics SB RAS, Novosibirsk 630090*
[4]*Faculty of Mathematics and Physics, Charles University, Prague 121 16*
[5]*Chonnam National University, Gwangju 61186*
[6]*University of Cincinnati, Cincinnati, Ohio 45221*
[7]*Deutsches Elektronen-Synchrotron, Hamburg 22607*
[8]*Duke University, Durham, North Carolina 27708*
[9]*University of Florida, Gainesville, Florida 32611*
[10]*Key Laboratory of Nuclear Physics and Ion-beam Application (MOE) and Institute of Modern Physics, Fudan University, Shanghai 200443*
[11]*II. Physikalisches Institut, Georg-August-Universität Göttingen, 37073 Göttingen*
[12]*SOKENDAI (The Graduate University for Advanced Studies), Hayama 240-0193*
[13]*Gyeongsang National University, Jinju 52828*
[14]*Department of Physics and Institute of Natural Sciences, Hanyang University, Seoul 04763*
[15]*University of Hawaii, Honolulu, Hawaii 96822*
[16]*High Energy Accelerator Research Organization (KEK), Tsukuba 305-0801*
[17]*J-PARC Branch, KEK Theory Center, High Energy Accelerator Research Organization (KEK), Tsukuba 305-0801*
[18]*Forschungszentrum Jülich, Jülich 52425*
[19]*IKERBASQUE, Basque Foundation for Science, Bilbao 48013*
[20]*Indian Institute of Science Education and Research Mohali, SAS Nagar, 140306*
[21]*Indian Institute of Technology Bhubaneswar, Satya Nagar 751007*
[22]*Indian Institute of Technology Guwahati, Assam 781039*
[23]*Indian Institute of Technology Hyderabad, Telangana 502285*

[24]*Indian Institute of Technology Madras, Chennai 600036*
[25]*Indiana University, Bloomington, Indiana 47408*
[26]*Institute of High Energy Physics, Chinese Academy of Sciences, Beijing 100049*
[27]*Institute of High Energy Physics, Vienna 1050*
[28]*INFN - Sezione di Napoli, Napoli 80126*
[29]*INFN - Sezione di Torino, Torino 10125*
[30]*Advanced Science Research Center, Japan Atomic Energy Agency, Naka 319-1195*
[31]*J. Stefan Institute, Ljubljana 1000*
[32]*Institut für Experimentelle Teilchenphysik, Karlsruher Institut für Technologie, Karlsruhe 76131*
[33]*Kennesaw State University, Kennesaw, Georgia 30144*
[34]*King Abdulaziz City for Science and Technology, Riyadh 11442*
[35]*Department of Physics, Faculty of Science, King Abdulaziz University, Jeddah 21589*
[36]*Kitasato University, Sagamihara 252-0373*
[37]*Korea Institute of Science and Technology Information, Daejeon 34141*
[38]*Korea University, Seoul 02841*
[39]*Kyungpook National University, Daegu 41566*
[40]*LAL, Université Paris-Sud, CNRS/IN2P3, Université Paris-Saclay, Orsay 91898*
[41]*École Polytechnique Fédérale de Lausanne (EPFL), Lausanne 1015*
[42]*P. N. Lebedev Physical Institute of the Russian Academy of Sciences, Moscow 119991*
[43]*Faculty of Mathematics and Physics, University of Ljubljana, Ljubljana 1000*
[44]*Ludwig Maximilians University, Munich 80539*
[45]*Luther College, Decorah, Iowa 52101*
[46]*University of Maribor, Maribor 2000*
[47]*Max-Planck-Institut für Physik, Munich 80805*
[48]*School of Physics, University of Melbourne, Victoria 3010*
[49]*University of Mississippi, University, Mississippi 38677*
[50]*Moscow Physical Engineering Institute, Moscow 115409*
[51]*Moscow Institute of Physics and Technology, Moscow Region 141700*
[52]*Graduate School of Science, Nagoya University, Nagoya 464-8602*
[53]*Kobayashi-Maskawa Institute, Nagoya University, Nagoya 464-8602*
[54]*Università di Napoli Federico II, 80055 Napoli*
[55]*Nara Women's University, Nara 630-8506*
[56]*National Central University, Chung-li 32054*
[57]*National United University, Miao Li 36003*
[58]*Department of Physics, National Taiwan University, Taipei 10617*
[59]*H. Niewodniczanski Institute of Nuclear Physics, Krakow 31-342*
[60]*Nippon Dental University, Niigata 951-8580*
[61]*Niigata University, Niigata 950-2181*
[62]*Novosibirsk State University, Novosibirsk 630090*
[63]*Osaka City University, Osaka 558-8585*
[64]*Pacific Northwest National Laboratory, Richland, Washington 99352*
[65]*Panjab University, Chandigarh 160014*
[66]*University of Pittsburgh, Pittsburgh, Pennsylvania 15260*
[67]*Research Center for Nuclear Physics, Osaka University, Osaka 567-0047*
[68]*Theoretical Research Division, Nishina Center, RIKEN, Saitama 351-0198*
[69]*University of Science and Technology of China, Hefei 230026*
[70]*Showa Pharmaceutical University, Tokyo 194-8543*
[71]*Soongsil University, Seoul 06978*
[72]*Sungkyunkwan University, Suwon 16419*
[73]*School of Physics, University of Sydney, New South Wales 2006*
[74]*Department of Physics, Faculty of Science, University of Tabuk, Tabuk 71451*
[75]*Tata Institute of Fundamental Research, Mumbai 400005*
[76]*Department of Physics, Technische Universität München, Garching 85748*
[77]*Earthquake Research Institute, University of Tokyo, Tokyo 113-0032*
[78]*Department of Physics, University of Tokyo, Tokyo 113-0033*
[79]*Tokyo Metropolitan University, Tokyo 192-0397*
[80]*Virginia Polytechnic Institute and State University, Blacksburg, Virginia 24061*

[81]*Wayne State University, Detroit, Michigan 48202*
[82]*Yamagata University, Yamagata 990-8560*
[83]*Yonsei University, Seoul 03722*

(Received 13 December 2019; accepted 2 March 2020; published 25 March 2020)

Using a data sample of 772×10^6 $B\bar{B}$ pairs collected on the $\Upsilon(4S)$ resonance with the Belle detector at the KEKB asymmetric energy e^+e^- collider, we report the observation of $B^0 \to p\bar{p}\pi^+\pi^-$ and the first observation of $B^+ \to p\bar{p}\pi^+\pi^0$. We measure a decay branching fraction of $(0.83 \pm 0.17 \pm 0.17) \times 10^{-6}$ in $B^0 \to p\bar{p}\pi^+\pi^-$ for $M_{\pi^+\pi^-} < 1.22$ GeV/c^2 with a significance of 5.5 standard deviations. The contribution from $B^0 \to p\bar{p}K^0$ is excluded. We measure a decay branching fraction of $(4.58 \pm 1.17 \pm 0.67) \times 10^{-6}$ for $B^+ \to p\bar{p}\pi^+\pi^0$ with $M_{\pi^+\pi^0} < 1.3$ GeV/c^2 with a significance of 5.4 standard deviations. We study the difference of the $M_{p\bar{p}}$ distributions in $B^0 \to p\bar{p}\pi^+\pi^-$ and $B^+ \to p\bar{p}\pi^+\pi^0$.

DOI: 10.1103/PhysRevD.101.052012

Charmless B decays offer a good opportunity to find sizable CP violation due to interference between the $b \to s$ penguin and $b \to u$ tree processes. Such decays can reveal new physics if measured results deviate from Standard Model expectations. In the B-factory era, both Belle and *BABAR* have discovered large direct CP violation in the $B \to K\pi$ system [1–3]. The LHCb Collaboration reported evidence of direct CP violation in $B^+ \to p\bar{p}K^+$ [4]. Here and throughout the text, the inclusion of the charge-conjugate mode is implied unless otherwise stated. This rare baryonic B decay presumably proceeds via the $b \to s$ penguin process with some non-negligible $b \to u$ contribution. It is intriguing that the invariant mass of the $p\bar{p}$ system peaks near threshold [5], and in the $p\bar{p}$ rest frame, K^+ is produced preferably in the $\bar{p}$ direction [6]. Interestingly, this angular asymmetry is opposite to that observed in $B^+ \to p\bar{p}\pi^+$, which is presumably dominated by the $b \to u$ tree process [6]. Most of the baryonic B decays presumably proceed predominantly via the $b \to s$ process, except for $B^+ \to p\bar{p}\pi^+$ and $B^0 \to p\bar{p}\pi^0$ [7] decays. It is important to measure other $b \to u$ baryonic B decays to provide more information for theoretical investigation based on a generalized factorization approach [8]. $B^0 \to p\bar{p}\pi^+\pi^-$ has been observed by LHCb [9], but there is still no observation for $B^+ \to p\bar{p}\pi^+\pi^0$.

We report a study of both $B^0 \to p\bar{p}\pi^+\pi^-$ and $B^+ \to p\bar{p}\pi^+\pi^0$ including the $B \to p\bar{p}\rho$ mass region using the full $\Upsilon(4S)$ dataset collected by the Belle detector [10,11] at the asymmetric energy e^+ (3.5 GeV) e^- (8 GeV) KEKB collider [12,13]. The data sample used in this study corresponds to an integrated luminosity of 711 fb^{-1}, which contains 772×10^6 $B\bar{B}$ pairs produced on the $\Upsilon(4S)$ resonance. The Belle detector surrounds the interaction point of KEKB. It is a large-solid-angle magnetic spectrometer that consists of a silicon vertex detector, a 50-layer central drift chamber (CDC), an array of aerogel threshold Cherenkov counters (ACC), a barrel-like arrangement of time-of-flight scintillation counters (TOF), and an electromagnetic calorimeter (ECL) comprised of CsI(Tl) crystals located inside a superconducting solenoid coil that provides a 1.5 T magnetic field. An iron flux return located outside of the coil is instrumented to detect K_L^0 mesons and identify muons.

For the study of $B \to p\bar{p}\pi\pi$, samples simulated with the Monte Carlo technique (MC) are used to optimize the signal selection criteria and estimate the signal reconstruction efficiency. These samples are generated with EvtGen [14] and a GEANT-based software package [15] to model the detector response. We generate the signal MC sample by a phase space model reweighted with the $p\bar{p}$ mass distribution obtained by LHCb [9] on $B^0 \to p\bar{p}\pi^+\pi^-$. The background samples include the continuum events ($e^+e^- \to u\bar{u}$, $d\bar{d}$, $s\bar{s}$, and $c\bar{c}$), generic B decays ($b \to c$), and rare B decays ($b \to u, d, s$). These simulated background samples are 6 times larger than the integrated luminosity of the accumulated Belle data.

We require charged particles to originate within a 2.0 cm region along the beam and from a 0.3 cm region on the transverse plane around the interaction region. To identify charged particles, we utilize the likelihood information determined for each particle type by the CDC, TOF, and ACC and apply the same selection criteria listed in Ref. [6] to select $p(\bar{p})$ and $\pi^+(\pi^-)$. The π^0 is reconstructed from two photons with a minimum energy in the laboratory frame of 0.05 GeV measured by the ECL. To reduce combinatoric background, the π^0 energy is required to be greater than 0.5 GeV, and the reconstructed mass is in the range $0.111 < M_{\gamma\gamma} < 0.151$ GeV/c^2, which corresponds to a ± 3.0 standard deviation (σ) window. We then perform a mass-constrained fit to the nominal π^0 mass [16] in order

Published by the American Physical Society under the terms of the Creative Commons Attribution 4.0 International license. Further distribution of this work must maintain attribution to the author(s) and the published article's title, journal citation, and DOI. Funded by SCOAP³.

to improve the resolution of the reconstructed π^0 four-momentum. To reject $B \to p\bar{p}D^{(*)}$ events, we restrict the invariant $\pi\pi$ mass $M_{\pi\pi}$ to be less than 1.22 GeV/c^2 for $B^0 \to p\bar{p}\pi^+\pi^-$ and 1.3 GeV/c^2 for $B^+ \to p\bar{p}\pi^+\pi^0$ based on studies of the simulated background. We use $\Delta E = E^*_{\rm recon} - E^*_{\rm beam}$ and $M_{\rm bc} = \sqrt{(E^*_{\rm beam}/c^2)^2 - (P^*_{\rm recon}/c)^2}$ to identify B decays. $E^*_{\rm recon}/P^*_{\rm recon}$ and $E^*_{\rm beam}$ are the reconstructed B energy/momentum and the beam energy measured in the $\Upsilon(4S)$ rest frame, respectively. For further investigation, we keep candidates with $5.24 < M_{\rm bc} < 5.29$ GeV/c^2 and $|\Delta E| < 0.2$ GeV.

We have further applied a D veto to reject candidate events with a charged pion, assumed to be a charged kaon, satisfying $|M_{K\pi} - M_D| < 0.4$ GeV/c^2. We require only one B candidate in each event. We choose the candidate with the smallest value of χ^2 in the B vertex fit. The fractions of $B^0 \to p\bar{p}\pi^+\pi^-$ and $B^+ \to p\bar{p}\pi^+\pi^0$ MC events with multiple B candidates are 16.4% and 20.3%, respectively. This selection removes 5.6% of the $B^0 \to p\bar{p}\pi^+\pi^-$ and 8.7% of the $B^+ \to p\bar{p}\pi^+\pi^0$ signal.

Based on the MC simulation, there are only a few events from generic or rare B decays in the candidate region ($5.24 < M_{\rm bc} < 5.29$ GeV/c^2 and $|\Delta E| < 0.2$ GeV); thus, they are ignored. The continuum background is the dominant component in the candidate region. Variables describing event topology are used to distinguish spherical $B\bar{B}$ events from jetlike continuum events. We use a neural network package, NeuroBayes [17], to separate the B signal from the continuum background. There are 28 input parameters for the neural network training, of which 23 parameters are modified Fox-Wolfram moments of particles of the signal B candidate, and separately those of particles in the rest of the event [18,19]. The remaining five parameters are the separation between the B candidate vertex and the accompanying B vertex along the longitudinal direction, the angle between the B flight direction and the beam axis in the $\Upsilon(4S)$ rest frame, the angle between the B momentum and the thrust axis of the event in the $\Upsilon(4S)$ rest frame, the sphericity [20] of the event calculated in the $\Upsilon(4S)$ rest frame, and the B flavor tagging quality parameter [21].

The output of NeuroBayes, $C_{\rm nb}$, ranges from -1 to $+1$, where the value is close to $+1$ for $B\bar{B}$-like and close to -1 for continuum-like events. We require the $C_{\rm nb}$ to be greater than 0.9 (0.87) for $B^0 \to p\bar{p}\pi^+\pi^-$ ($B^+ \to p\bar{p}\pi^+\pi^0$) with optimizations based on a figure of merit (FOM) defined as

$$\mathrm{FOM} = \frac{N_{\rm s}}{\sqrt{N_{\rm s} + N_{\rm b}}}, \tag{1}$$

where $N_{\rm s}$ is the expected signal yield, assuming the branching fraction measured by LHCb for $B^0 \to p\bar{p}\pi^+\pi^-$ and the same value for $B^+ \to p\bar{p}\pi^+\pi^0$, and $N_{\rm b}$ is the number of background events from the MC simulations. To extract the $B \to p\bar{p}\pi\pi$ yield for events in the candidate region, we perform an extended unbinned likelihood fit to variables ΔE and $M_{\rm bc}$. These variables are assumed to be uncorrelated. The fit function used is

$$\mathcal{L} = \frac{e^{-\Sigma_{j=1}^{2}(N_j)}}{N!} \prod_{i=1}^{N} \sum_{j} (N_j P_j(M^i_{\rm bc}, \Delta E^i)), \tag{2}$$

where N is the number of total events, i denotes the event index, j stands for the component index (signal or background), and P represents the probability density function (PDF).

To model the signal distributions, we use double Gaussian functions for ΔE of $B^0 \to p\bar{p}\pi^+\pi^-$, a Crystal Ball function [22] and a Gaussian function for ΔE of $B^+ \to p\bar{p}\pi^+\pi^0$, and a double Gaussian function for $M_{\rm bc}$. For the background, we use a second-order Chebyshev polynomial function and an ARGUS function [23] to describe ΔE and $M_{\rm bc}$, respectively. The signal distributions in ΔE and $M_{\rm bc}$ are calibrated with $B^0 \to p\bar{p}\bar{D}^0$ ($\bar{D}^0 \to K^+\pi^-$) and $B^0 \to \bar{D}^0\pi^0$ ($\bar{D}^0 \to K^+\pi^-$) by comparing the shape difference between the predictions of the MC and data. These modes have the same multiplicity in the final state as our signal, much larger statistics, and small backgrounds. We fix the calibrated signal shapes from MC simulation and allow the component yields and all other PDF shape parameters to float. The fit results are shown in Figs. 1 and 2.

We find the signal yields of $B^0 \to p\bar{p}\pi^+\pi^-$ and $B^+ \to p\bar{p}\pi^+\pi^0$ to be $73.8^{+15.8}_{-14.9}$ and 151 ± 39 with fit significances of 5.5σ and 5.4σ, respectively. The significance is defined as $\sqrt{-2 \times \ln(\mathcal{L}_0/\mathcal{L}_s)}(\sigma)$, where $\mathcal{L}_0$ is the likelihood with zero signal yield and $\mathcal{L}_s$ is the likelihood for the measured yield. In this calculation, we have used the likelihood function which is smeared by including the additive systematic uncertainties that affect the yield. With the large significance of both modes, we then measure the signal yields in different $M_{\pi\pi}$ bins with the same fit method. Table I and Fig. 3 show the yield and statistical significance in different $M_{\pi\pi}$ bins for $B^0 \to p\bar{p}\pi^+\pi^-$; Table II and Fig. 4 show them for $B^+ \to p\bar{p}\pi^+\pi^0$. For $B^0 \to p\bar{p}\pi^+\pi^-$, signal events in the bin $0.46 < M_{\pi\pi} < 0.53$ GeV/c^2 are mostly from $B^0 \to p\bar{p}K^0_S$, and hence we exclude this range in the contribution shown in Table I and Fig. 3, and from the measurement of $\mathcal{B}(B^0 \to p\bar{p}\pi^+\pi^-)$. Assuming the $\Upsilon(4S)$ decays to charged and neutral $B\bar{B}$ pairs equally, we use the efficiency obtained from the MC simulation and fitted signal yield to calculate the branching fraction. After calculating overall efficiencies for $B^0 \to p\bar{p}\pi^+\pi^-$ and $B^+ \to p\bar{p}\pi^+\pi^0$, the branching fractions of $B^0 \to p\bar{p}\pi^+\pi^-$ and $B^+ \to p\bar{p}\pi^+\pi^0$ for $M_{\pi^+\pi^-} < 1.22$ GeV/c^2 and $M_{\pi^+\pi^0} < 1.3$ GeV/c^2 are found to be $(0.83 \pm 0.17 \pm 0.17) \times 10^{-6}$ and $(4.58 \pm 1.17 \pm 0.67) \times 10^{-6}$; the signal efficiencies are 11.5% and 4.3%, respectively.

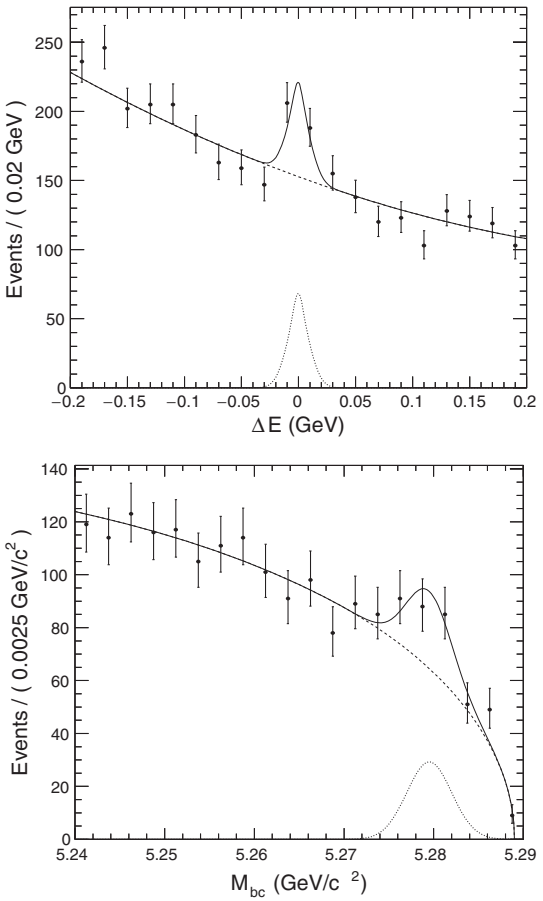

FIG. 1. Fit results of $B^0 \to p\bar{p}\pi^+\pi^-$ projected onto ΔE (with $5.27 < M_{\rm bc} < 5.29\,{\rm GeV}/c^2$) and $M_{\rm bc}$ (with $-0.03 < \Delta E < 0.03$ GeV). The dashed line represents the background. The dotted line represents the signal. The solid line is the sum of all fit components.

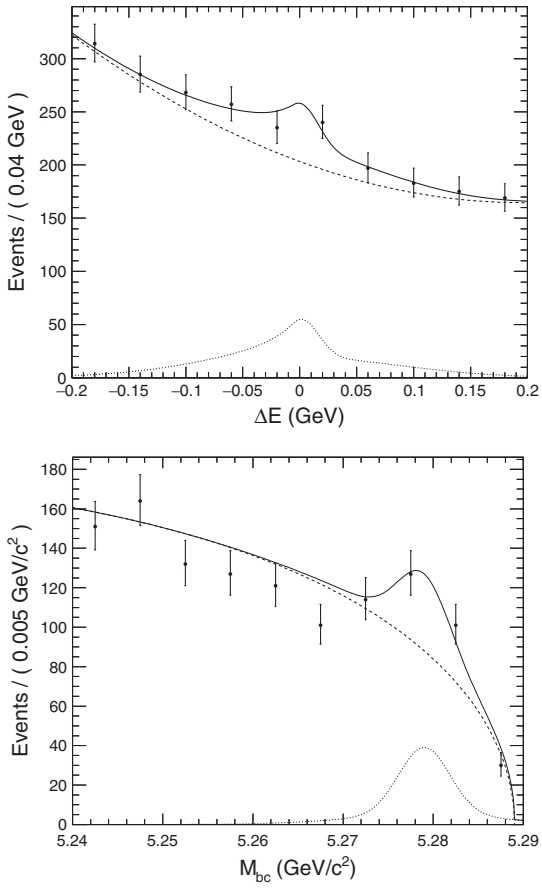

FIG. 2. Fit results of $B^+ \to p\bar{p}\pi^+\pi^0$ projected onto ΔE (with $5.27 < M_{\rm bc} < 5.29\,{\rm GeV}/c^2$) and $M_{\rm bc}$ (with $-0.03 < \Delta E < 0.03$ GeV). The dashed line represents the background. The dotted line represents the signal. The solid line is the sum of all fit components.

We attempted to find the contribution of $B^+ \to p\bar{p}\rho^+$ by minimizing the χ^2 between the observed data and the assumed nonresonant $B^+ \to p\bar{p}\pi^+\pi^0$ and $B^+ \to p\bar{p}\rho^+$ decays. To describe the $M_{\pi\pi}$ distribution, we use the phase space model for nonresonant $B^+ \to p\bar{p}\pi^+\pi^0$ and a Breit-Wigner function convolved with a Gaussian function for $B^+ \to p\bar{p}\rho^+$. We set the Breit-Wigner function with its mean and width to the nominal values for the ρ^+ convolved with a Gaussian resolution function of 5 MeV/c^2 width. The result is shown in Fig. 4.

The fit gives a yield of 86 ± 41 events with a $\frac{\chi^2}{n_{\rm dof}}$ of 17.0/11 for $B^+ \to p\bar{p}\rho^+$. Our current data sample is not large enough to separate the contributions of $B^+ \to p\bar{p}\rho^+$ and nonresonant $B^+ \to p\bar{p}\pi^+\pi^0$. The measured $\mathcal{B}(B^+ \to p\bar{p}\pi^+\pi^0)$ with $B^+ \to p\bar{p}\rho^+$ included is almost a factor of 10 smaller than the predicted $\mathcal{B}(B^+ \to p\bar{p}\rho^+)$ [8].

There are modes sharing the same final-state particles as our signal, such as $B \to \bar{p}\Delta^{++}\pi$ or $B \to \bar{p}\Lambda^0\pi$. Examining the $M_{\Delta(p\pi^+)}$ and $M_{\Lambda(p\pi^-)}$ spectra, we find no obvious contribution from these modes.

TABLE I. Yields, statistical significance, and efficiencies ($\varepsilon_{\rm eff}$) in different $M_{\pi\pi}$ bins for $B^0 \to p\bar{p}\pi^+\pi^-$.

$M_{\pi\pi}$ (GeV/c^2)	N_s	σ	$\varepsilon_{\rm eff}$ (%)
$M_{\pi\pi} < 0.39$	$-2.7^{+3.9}_{-3.0}$	...	11.2
0.39–0.46	$9.5^{+5.9}_{-5.0}$	2.1	11.5
0.46–0.53	K^0_S veto	...	...
0.53–0.6	$-0.1^{+3.9}_{-3.1}$	...	11.3
0.6–0.67	$1.9^{+4.9}_{-4.4}$	0.5	11.9
0.67–0.74	$10.8^{+6.7}_{-5.8}$	2.0	12.1
0.74–0.81	$13.0^{+6.5}_{-5.6}$	2.6	12.3
0.81–0.88	$13.9^{+6.1}_{-5.3}$	3.1	11.8
0.88–0.95	$16.5^{+6.0}_{-5.3}$	4.1	10.8
0.95–1.02	$0.5^{+2.6}_{-2.1}$	...	9.6
1.02–1.09	$3.6^{+4.0}_{-3.1}$	1.2	8.4
1.09–1.16	$1.2^{+3.2}_{-2.8}$	0.5	6.5
1.16–1.22	$2.3^{+2.9}_{-1.9}$	1.3	3.5

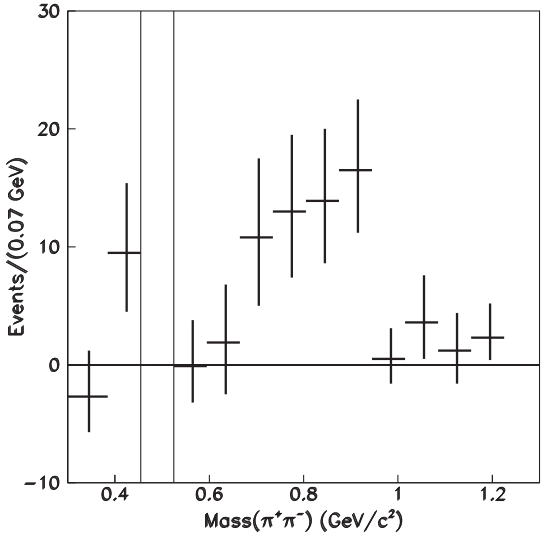

FIG. 3. The $M_{\pi\pi}$ signal distribution for $B^0 \to p\bar{p}\pi^+\pi^-$.

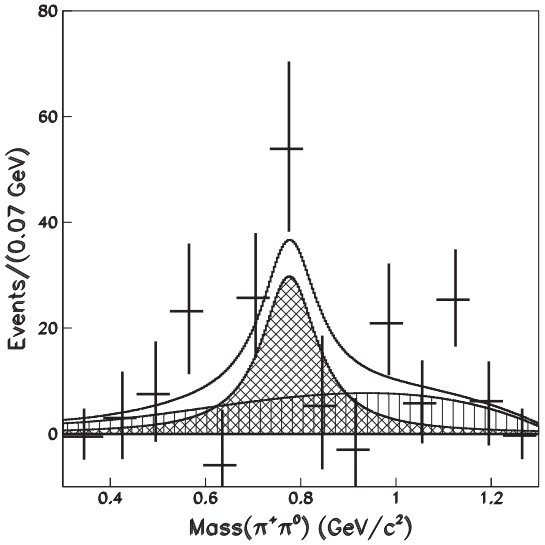

FIG. 4. Fit results of $B^+ \to p\bar{p}\pi^+\pi^0$ in different $M_{\pi\pi}$ bins. The cross-hatched region represents the $B^+ \to p\bar{p}\rho^+$ component, and the vertical-line-hatched region represents the $B^+ \to p\bar{p}\pi^+\pi^0$ component.

We investigate the $M_{p\bar{p}}$ distribution of B signals in three regions: $M_{p\bar{p}} < 2.85$ GeV/c^2 for the threshold enhancement region, $2.85 < M_{p\bar{p}} < 3.128$ GeV/c^2 for the charmonium-enhanced region, and 3.128 GeV/$c^2 < M_{p\bar{p}}$ for the phase-space-dominant region. We perform a 2D $(\Delta E, M_{\rm bc})$ likelihood fit to extract the signal yields of the $B \to p\bar{p}\pi\pi$ decays in each region.

Tables III and IV show the fitted yields with statistical fit significances for $B^0 \to p\bar{p}\pi^+\pi^-$ and $B^+ \to p\bar{p}\pi^+\pi^0$, respectively. The charmonium-enhanced region, $2.85 < M_{p\bar{p}} < 3.128$ GeV/c^2, includes other expected resonant modes such as $B \to J/\psi\rho$ [16]. We find that $B^0 \to p\bar{p}\pi^+\pi^-$ events are equally distributed in the bins below and above the charmonium-enhanced region, while $B^+ \to p\bar{p}\pi^+\pi^0$ events are dominant in the bin below the charmonium-enhanced region. We also calculated the branching fraction of $B^0 \to p\bar{p}\pi^+\pi^-$ in the threshold enhancement region to be $(0.35 \pm 0.13 \pm 0.07) \times 10^{-6}$, which is consistent with the observed result from LHCb [9]. Sources of systematic uncertainties are summarized in Table V. The number of $B\bar{B}$ pairs is known to within 1.4%. By using the partially reconstructed $D^{*+} \to D^0\pi^+$ with $D^0 \to \pi^+\pi^- K^0_S$ events, the uncertainty due to the charged-track reconstruction

TABLE II. Yields, statistical significance, and efficiencies ($\varepsilon_{\rm eff}$) in different $M_{\pi\pi}$ bins for $B^+ \to p\bar{p}\pi^+\pi^0$.

$M_{\pi\pi}$ (GeV/c^2)	N_s	σ	$\varepsilon_{\rm eff}$ (%)
$M_{\pi\pi} < 0.39$	$-0.5^{+5.3}_{-4.4}$	⋯	4.3
0.39–0.46	$3.0^{+8.8}_{-7.8}$	0.3	4.1
0.46–0.53	$7.5^{+10.0}_{-9.0}$	0.8	4.9
0.53–0.6	$23.2^{+12.8}_{-11.9}$	2.2	4.7
0.6–0.67	$-5.9^{+10.5}_{-9.2}$	⋯	4.8
0.67–0.74	$25.7^{+12.3}_{-11.4}$	1.8	5.0
0.74–0.81	$53.9^{+16.5}_{-15.7}$	3.7	5.1
0.81–0.88	$5.3^{+13.3}_{-12.0}$	0.4	4.8
0.88–0.95	$-3.0^{+9.8}_{-8.5}$	⋯	4.3
0.95–1.02	$20.9^{+11.3}_{-9.8}$	1.7	3.7
1.02–1.09	$5.8^{+8.1}_{-7.6}$	0.8	2.7
1.09–1.16	$25.4^{+9.5}_{-8.7}$	3.1	2.7
1.16–1.23	$6.2^{+7.5}_{-8.4}$	0.8	2.2
1.23–1.3	$-0.3^{+5.3}_{-4.5}$	⋯	0.8

TABLE III. Yields, statistical significance, and efficiencies ($\varepsilon_{\rm eff}$) in different $M_{p\bar{p}}$ bins for $B^0 \to p\bar{p}\pi^+\pi^-$ ($0.6 < M_{\pi\pi} < 1.22$ GeV/c^2).

$M_{p\bar{p}}$ (GeV/c^2)	N_s	σ	$\varepsilon_{\rm eff}$ (%)
$M_{p\bar{p}} < 2.85$	$26.1^{+10.0}_{-9.1}$	4.0	9.8
$2.85 < M_{p\bar{p}} < 3.128$	$19.6^{+10.2}_{-9.3}$	2.9	9.9
$3.128 < M_{p\bar{p}}$	$29.1^{+16.2}_{-13.1}$	3.5	9.4

TABLE IV. Yields, statistical significance, and efficiencies ($\varepsilon_{\rm eff}$) in different $M_{p\bar{p}}$ bins for $B^+ \to p\bar{p}\pi^+\pi^0$ ($M_{\pi\pi} < 1.3$ GeV/c^2).

$M_{p\bar{p}}$ (GeV/c^2)	N_s	σ	$\varepsilon_{\rm eff}$ (%)
$M_{p\bar{p}} < 2.85$	$133.5^{+26.6}_{-25.2}$	5.1	4.8
$2.85 < M_{p\bar{p}} < 3.128$	$12.3^{+10.3}_{-9.7}$	1.4	4.0
$3.128 < M_{p\bar{p}}$	$-3.8^{+15.1}_{-13.8}$	⋯	3.4

TABLE V. Table of systematic uncertainties (%) for $B^0 \to p\bar{p}\pi^+\pi^-$ and $B^+ \to p\bar{p}\pi^+\pi^0$.

Uncertainties	$B^0 \to p\bar{p}\pi^+\pi^-$	$B^+ \to p\bar{p}\pi^+\pi^0$
$N_{B\bar{B}}$	1.4	1.4
Tracking	1.4	1.1
p/π identification	3.3	2.4
π^0 reconstruction	...	2.8
Continuum suppression	4.7	4.3
Decay model	14.3	8.6
ΔE, $M_{\rm bc}$ shape	12.4	10.4
Summary	19.9	14.6

efficiency is estimated to be 0.35% per track. We use a $\Lambda \to p\pi^-$ ($D^{*+} \to D^0\pi^+$, $D^0 \to K^-\pi^+$) sample to calibrate the MC p (π^+) identification efficiency and assign uncertainties of 3.3% and 2.4% for $B^0 \to p\bar{p}\pi^+\pi^-$ and $B^+ \to p\bar{p}\pi^+\pi^0$ decays, respectively. For π^0 reconstruction, we determine its uncertainty by using a $\tau^- \to \pi^-\pi^0\nu$ data sample [24]. To estimate the systematic error due to continuum suppression, we use the $B^0 \to p\bar{p}\bar{D}^0$ and $B^0 \to \bar{D}^0\pi^0$ data/MC samples, where $\bar{D}^0 \to K^+\pi^-$. We choose the efficiency of the phase space model for $B^0 \to p\bar{p}\pi^+\pi^-$ and the efficiency of the reweighted phase space model for $B^+ \to p\bar{p}\pi^+\pi^0$, and we estimate the efficiency uncertainty as a difference of signal efficiencies for $B^0 \to p\bar{p}\pi^+\pi^-$ in the reweighted phase space model and $B^+ \to p\bar{p}\pi^+\pi^0$ in the phase space model. The uncertainty associated with the parameters of the ΔE and $M_{\rm bc}$ PDFs is examined by repeating the fit with each parameter varied by 1 standard deviation from its nominal value. The assumption of no correlation between ΔE and $M_{\rm bc}$ is examined by replacing the PDF of B signal events with the corresponding 2D histogram function.

In summary, we report the observation of $B^0 \to p\bar{p}\pi^+\pi^-$ and the first observation of $B^+ \to p\bar{p}\pi^+\pi^0$ with branching fractions of $(0.83 \pm 0.17 \pm 0.17) \times 10^{-6}$ and $(4.58 \pm 1.17 \pm 0.67) \times 10^{-6}$ for $M_{\pi^+\pi^-} < 1.22\ {\rm GeV}/c^2$ and $M_{\pi^+\pi^0} < 1.3\ {\rm GeV}/c^2$, respectively. In contrast to the theoretical prediction [8], the measured $\mathcal{B}$ for $B^+ \to p\bar{p}\pi^+\pi^0$ in the ρ-enhanced region is an order of magnitude smaller than the theoretical expectation. Similar deviation from the theoretical expectation has also been found in $B^+ \to p\bar{p}\mu^+\nu_\mu$ by LHCb [25] and Belle [26]. We find that the $B^+ \to p\bar{p}\pi^+\pi^0$ decay should be dominated by the lower $M_{p\bar{p}}$ bin, which is not the case in the $B^0 \to p\bar{p}\pi^+\pi^-$ decay. These findings are useful for future theoretical investigation.

ACKNOWLEDGMENTS

We thank the KEKB group for the excellent operation of the accelerator, the KEK cryogenics group for the efficient operation of the solenoid, the KEK computer group and the Pacific Northwest National Laboratory (PNNL) Environmental Molecular Sciences Laboratory (EMSL) computing group for strong computing support, and the National Institute of Informatics and Science Information NETwork 5 (SINET5) for valuable network support. We acknowledge support from the Ministry of Education, Culture, Sports, Science, and Technology (MEXT) of Japan, the Japan Society for the Promotion of Science (JSPS), and the Tau-Lepton Physics Research Center of Nagoya University; the Australian Research Council including Grants No. DP180102629, No. DP170102389, No. DP170102204, No. DP150103061, and No. FT130100303; the Austrian Science Fund (FWF); the National Natural Science Foundation of China under Contracts No. 11435013, No. 11475187, No. 11521505, No. 11575017, No. 11675166, and No. 11705209; the Key Research Program of Frontier Sciences, Chinese Academy of Sciences (CAS), Grant No. QYZDJ-SSW-SLH011; the CAS Center for Excellence in Particle Physics (CCEPP); the Shanghai Pujiang Program under Grant No. 18PJ1401000; the Ministry of Education, Youth and Sports of the Czech Republic under Contract No. LTT17020; the Carl Zeiss Foundation, the Deutsche Forschungsgemeinschaft, the Excellence Cluster Universe, and the VolkswagenStiftung; the Department of Science and Technology of India; the Istituto Nazionale di Fisica Nucleare of Italy; the National Research Foundation (NRF) of Korea under Grants No. 2015H1A2A1033649, No. 2016R1D1A1B01010135, No. 2016K1A3A7A09005603, No. 2016R1D1A1B02012900, No. 2018R1A2B3003643, No. 2018R1A6A1A06024970, and No. 2018R1D1A1B07047294; the Radiation Science Research Institute, Foreign Large-size Research Facility Application Supporting project, the Global Science Experimental Data Hub Center of the Korea Institute of Science and Technology Information and KREONET/GLORIAD; the Polish Ministry of Science and Higher Education and the National Science Center; the Grant of the Russian Federation Government, Agreement No. 14.W03.31.0026; the Slovenian Research Agency; Ikerbasque, Basque Foundation for Science, Spain; the Swiss National Science Foundation; the Ministry of Education and the Ministry of Science and Technology of Taiwan; and the United States Department of Energy and the National Science Foundation.

[1] H. Ishino *et al.* (Belle Collaboration), Phys. Rev. Lett. **98**, 211801 (2007).
[2] B. Aubert *et al.* (*BABAR* Collaboration), Phys. Rev. Lett. **99**, 021603 (2007).
[3] S. Lin *et al.* (Belle Collaboration), Nature (London) **452**, 332 (2008).
[4] R. Aaij *et al.* (LHCb Collaboration), Phys. Rev. Lett. **113**, 141801 (2014).
[5] K. Abe *et al.* (Belle Collaboration), Phys. Rev. Lett. **88**, 181803 (2002).
[6] J. Wei *et al.* (Belle Collaboration), Phys. Lett. B **659**, 80 (2008).
[7] B. Pal *et al.* (Belle Collaboration), Phys. Rev. D **99**, 091104 (2019).
[8] C. Q. Geng, Y. K. Hsiao, and J. N. Ng, Phys. Rev. D **75**, 094013 (2007).
[9] R. Aaij *et al.* (LHCb Collaboration), Phys. Rev. D **96**, 051103 (2017).
[10] A. Abashian *et al.* (Belle Collaboration), Nucl. Instrum. Methods Phys. Res., Sect. A **479**, 117 (2002).
[11] J. Brodzicka *et al.*, Prog. Theor. Exp. Phys. **2012**, 04D001 (2012).
[12] S. Kurokawa and E. Kikutani, Nucl. Instrum. Methods Phys. Res., Sect. A **499**, 1 (2003), and other papers included in this volume.
[13] T. Abe *et al.*, Prog. Theor. Exp. Phys. **2013**, 03A001 (2013).
[14] D. Lange, Nucl. Instrum. Methods Phys. Res., Sect. A **462**, 152 (2001).
[15] R. Brun *et al.*, CERN Report No. DD/EE/84-1, 1984.
[16] M. Tanabashi *et al.* (Particle Data Group), Phys. Rev. D **98**, 030001 (2018).
[17] M. Feindt and U. Kerzel, Nucl. Instrum. Methods Phys. Res., Sect. A **559**, 190 (2006).
[18] G. Fox and S.Wolfram, Phys. Rev. Lett. **41**, 1581 (1978).
[19] S. Lee *et al.* (Belle Collaboration), Phys. Rev. Lett. **91**, 261801 (2003).
[20] J. Bjorken and S. Brodsky, Phys. Rev. D **1**, 1416 (1970).
[21] H. Kakuno *et al.* (Belle Collaboration), Nucl. Instrum. Methods Phys. Res., Sect. A **533**, 516 (2004).
[22] T. Skwarnicki, Ph.D. thesis, Institute for Nuclear Physics, and DESY, 1986.
[23] H. Albrecht *et al.* (ARGUS Collaboration), Phys. Lett. B **241**, 278 (1990).
[24] S. Ryu *et al.* (Belle Collaboration), Phys. Rev. D **89**, 072009 (2014).
[25] R. Aaij *et al.* (LHCb Collaboration), CERN Report No. LHCb-PAPER 034, 2019, https://arxiv.org/abs/1911.08187.
[26] K.-J. Tien *et al.* (Belle Collaboration), Phys. Rev. D **89**, 011101 (2014).